JOURNAL OF VIROLOGY, Dec. 1992, p. 6849–6857
0022-538X/92/126849-09$02.00/0

Vol. 66, No. 12

Myristate-Protein Interactions in Poliovirus: Interactions of VP4 Threonine 28 Contribute to the Structural Conformation of Assembly Intermediates and the Stability of Assembled Virions

NICOLA MOSCUFO AND MARIE CHOW*

Department of Biology, Massachusetts Institute of Technology, Cambridge, Massachusetts 02139

Received 1 July 1992/Accepted 18 August 1992

The VP4 capsid protein of poliovirus is N-terminally modified with myristic acid. Within the poliovirus structure, a hydrogen bond is observed between the myristate carbonyl and the hydroxyl side chain of threonine 28 of VP4. This interaction is between two fivefold symmetry-related copies of VP4 and is one of several myristoyl-mediated interactions that appears to structurally link the promoters within the pentamer subunit of the virus particle. Site-specific substitutions of the threonine residue were constructed to investigate the biological relevance of these myristate-protein interactions. Replacement of the threonine with glycine or lysine is lethal, generating nonviable viruses. Substitution with serine or valine led to viable viruses, but these mutants displayed anomalies during virus assembly. In addition, both assembled serine- and valine-substituted virion particles showed reduced infectivity and were more sensitive to thermal inactivation and antibody neutralization. Thus the threonine residue provides interactions necessary for efficient assembly of the virus and for virion stability.

Poliovirus, the causative agent of poliomyelitis in humans, is a picornavirus. The icosahedrally symmetric virion is formed from 60 copies of each of four proteins, VP1, VP2, VP3, and VP4, and encapsidates a positive-stranded RNA genome of approximately 7,500 nucleotides. One structural feature common to most picornaviruses is the modification of the N-terminal glycine residue of VP4 subunits with myristic acid (the saturated tetradecanoic fatty acid) (2). In poliovirus, this cotranslationally added covalent modification is required for formation of the infectious particle (11, 12, 21), and two stages have been identified during virus assembly in which this modification is critical (14).

Initially, the capsid proteins are synthesized within the infected cell as a single translational unit, generating the myristoyl-modified 100-kDa capsid precursor (P1). Different stages of virion assembly are associated with specific cleavages of the capsid protein precursors. Thus, formation of pentamer intermediates appears to require cleavage of P1 to VP0-VP1-VP3, and in the final stages of virion assembly (conversion of the provirion to the mature virion), VP0 is cleaved to form capsid proteins VP4 and VP2 (18). A number of assembly intermediates have been identified in poliovirus-infected cells (18). These include the 5S uncleaved capsid precursor or protomer (P1), the 5S cleaved protomer (VP0-VP3-VP1), the 14S pentamer, the 73S native empty particle, and the provirion. During formation of the obligate pentamer intermediate, there is a kinetic preference for myristoylated cleaved protomers (VP0-VP3-VP1). Unmodified protomers can be incorporated into pentameric structures but may require the presence of modified protomers to nucleate the assembly reaction. Subsequently, pentamer and empty capsid assembly intermediates containing unmodified promoters are excluded from the later stages of virion morphogenesis: RNA encapsidation and maturation of the provirion (14). Further studies reveal no specific association of poliovirus assembly intermediates with intracellular membranes, and the myristoyl moiety does not serve as a membrane-targeting signal (10). Thus, observed functional effects of the myristoyl moiety during capsid assembly are mediated via protein-protein or myristate-protein interactions.

Presently, poliovirus is the only example in which myristate-mediated protein interactions are visible within a high-resolution atomic structure. The five myristoyl moieties are located around the fivefold axis within each pentamer substructure of the poliovirus virion (2, 7). The myristoyl molecule participates in a network of interactions that links the VP4 protein of any given protomer with VP3 and VP4 proteins of other fivefold-symmetry-related promoters. These interactions include a hydrogen bond that is formed between the carbonyl oxygen of the myristoyl molecule and the threonine at residue 28 (4028T) from an adjacent VP4 protein. The biological relevance of this noncovalent interaction was investigated by constructing mutant poliovirus genomes in which the 4028T residue was replaced with different amino acids. Characterization of the viable 4028T mutants indicates that substitution of threonine 28 affects the assembly and stability of the virus capsid. The observed mutant phenotypes suggest that the threonine side chain participates in several types of interactions.

MATERIALS AND METHODS

Methods for cell propagation, DEAE-dextran-mediated plasmid transfections, virus purification, determination of viral titers (PFUs), and viral growth curves were as previously described (14).

Nomenclature. In the virus nomenclature used in this study, the first number indicates the poliovirus capsid subunit and the following three digits indicate the amino acid position within the protein sequence. This number is followed by the single-letter code for the amino acid present in

* Corresponding author.

the wild-type parent strain followed by the letter for the amino acid substitution in the mutant (14). Thus 4028T.S identifies the poliovirus mutant in which the threonine at position 28 of capsid protein VP4 was replaced with a serine.

Plasmid and site-directed mutagenesis. pPVM1 contains an infectious cDNA copy of the poliovirus genome (serotype 1, Mahoney strain). The subcloning strategy and reconstruction of the mutant viral genomes are as previously described (14). Nucleotides 824 to 826 encode threonine 28 of VP4 (4028T). A synthetic 23-mer nucleotide complementary to the genomic sequence of nucleotides 813 to 835 was synthesized with a random combination of nucleotides at positions 824 to 826 (Massachusetts Institute of Technology biopolymer facility), and the oligonucleotide was incorporated (20). After the reconstitution of the mutated fragment within the full-length poliovirus cDNA genome, the sequences of the entire inserted fragment and the genome junctions for each constructed pPVM1 mutant were determined to confirm the location and identity of the nucleotide substitutions (19). The mutant pPVM1 plasmids were transfected into HeLa cells.

Propagation of viral stocks. Well-isolated plaques were picked from the pPVM1-transfected plates and placed in 1 ml of phosphate-buffered saline (PBS). The titers of these initial stocks were determined, and the viruses were used to infect HeLa cell monolayers at 37°C at low multiplicities of infection (MOI, 0.01 to 0.1). Infected cells and media were harvested after 2 to 3 days of incubation, and virus particles were released by freeze-thawing. The supernatants (10^8 to 10^9 PFU/ml) were stored as aliquots at −20°C. Cesium chloride-purified virus stocks were generated from these low-MOI virus stocks by a single high-multiplicity infection in HeLa cells (MOI, 10) and were used in all experiments. Virus was purified by standard procedures and stored at −20°C in 50 mM Tris-HCl (pH 7.5)–100 mM NaCl–0.1 mM EDTA (15). To confirm that these viruses still contained the constructed mutation, we determined the sequence encoding the VP4 protein in these purified viruses by direct dideoxynucleotide sequencing of the RNA genome with avian myeloblastosis virus reverse transcriptase (Life Sciences Inc.) (15).

Metabolic labeling of viral proteins. HeLa cells in suspension (4×10^6 cells per ml) were infected (MOI, 10) at 37°C in methionine-free minimal essential medium containing 5% fetal calf serum. Infected cells were labeled continuously at 37°C from 3.5 to 5.5 h postinfection (p.i.) with [^{35}S]methionine (final concentration, 40 μCi/ml; 1,100 Ci/mmol; NEN Dupont) and harvested. Pulse-chase experiments were done, and the infected-cell extracts were analyzed (14).

Sucrose gradient analysis. Infected HeLa cells labeled with [^{35}S]methionine were lysed in 500 μl of TNM (10 mM Tris-HCl [pH 7.5], 10 mM NaCl, 1.5 mM $MgCl_2$) containing 1% sodium deoxycholate, 1% Brij 58, and 0.05 mM phenylmethylsulfonyl fluoride and incubated at 4°C for 20 min. Cell nuclei were pelleted at $900 \times g$, and equal cell volumes of the resultant cell extract were analyzed on 6 to 25% and 15 to 30% sucrose gradients (14). The gradients were centrifuged at 4°C in an SW40 rotor for 16.5 h at 40,000 rpm (6 to 25% gradients) or for 2.5 h at 39,000 rpm (15 to 30% gradients). Fractions were collected from the top, and the radioactivity of each fraction was determined. Fractions at the desired sedimentation value were analyzed by polyacrylamide gel electrophoresis (9).

In vitro assembly of empty capsids from pentamers. Sucrose gradient fractions containing pentamers were pooled. The molar concentration of pentamers was determined from the protein content of the pooled sample by assuming a pentamer molecular mass of 485 kDa. The concentration of pentamers (in TNM buffer) in the in vitro assembly reactions was at least 16 nM; this concentration is 10-fold higher than the threshold concentration necessary for efficient self-assembly (17). Pentamers were incubated at either 4 or 37°C for 1 h and then analyzed on 10 to 30% sucrose gradients. The gradients were centrifuged at 4°C for 2 h in an SW50.1 rotor (50,000 rpm) and fractionated, and the radioactivity in each fraction was determined.

Dissociation of empty capsids at elevated pH. Guanidine-HCl (final concentration, 2 mM) was added to infected HeLa cells (MOI, 10) at 3 h p.i. to inhibit the viral RNA replication and induce accumulation of empty capsids (8). Cells were continuously labeled with [^{35}S]methionine from 3.5 to 5.5 h p.i. and harvested. The cells were lysed at either pH 7.5 or 8.3 in TNM buffer containing 1% sodium deoxycholate, 1% Brij 58, and 0.05 mM phenylmethylsulfonyl fluoride. Samples of cell extracts were loaded on 15 to 30% linear sucrose gradients in TNM at either at pH 7.5 or 8.3, respectively.

Thermostability of virus particles. CsCl-purified viruses (10^7 PFU/ml of PBS) were incubated in close-capped vials at 45°C. Aliquots (50 μl) were periodically removed, and the infectious titer remaining was determined by plaque assay (1).

Sensitivity to neutralizing MAbs. Monoclonal antibodies (MAbs) specific for neutralizing antigenic site 2 (MAbs 4 and 8), site 3A (MAbs 1 and 12), and site 3B (MAbs 10 and 13) were used in microneutralization assays (15). The MAbs were diluted in PBS containing 0.1% bovine serum albumin and placed in flat-bottomed 96-well tissue culture dishes (50 μl per well). Virus (5×10^4 PFU/50 μl of DME) was added to each well, and the wells were incubated at 37°C for 1 h. Subsequently, HeLa cells (5×10^4 cells per 50 μl) in RPMI 1640 containing 5% fetal calf serum were added to each well, and the wells were incubated at 37°C for 30 h. Viable cells were stained with crystal violet. The neutralizing titer of each MAb was determined as the dilution of MAb that protected the cell monolayer from lysis by the virus. Neutralization titers for a given MAb were always determined for both wild-type and mutant viruses within the same assay.

RESULTS

An intersubunit hydrogen bond within the infectious poliovirus virion is formed between the carbonyl oxygen of the myristoyl moiety and the hydroxyl component of the threonine at residue 28 (4028T) from an adjacent VP4 protein (2). To assess the biological importance of this hydrogen bond, we replaced the threonine 4028T by several amino acids (serine, valine, glycine, or lysine). Transfection of the full-length pPVM plasmids containing the glycine or lysine substitutions consistently failed to give plaques, and thus these substitutions are likely to be lethal for the virus. Substitution of the threonine residue with a serine would remove the methyl moiety of the side chain, but the intersubunit hydrogen bond could still be formed with the hydroxyl side chain. The valine substitution would replace the hydroxyl group with a methyl moiety and prevent hydrogen bond formation at this residue position. Surprisingly, viable mutants were recovered after transfection of HeLa cells with pPVM plasmids, containing either the serine or the valine substitution.

Characterization of 4028T.S and 4028T.V mutants. Both serine and valine mutants (4028T.S and 4028T.V) consistently displayed small-plaque phenotypes at all temperatures (Fig. 1). The replication efficiencies of the 4028T.S and

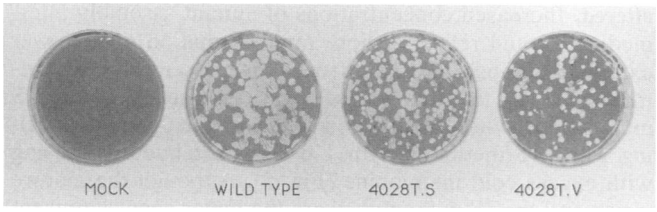

FIG. 1. Plaque phenotypes of wild-type, 4028T.S, and 4028T.V polioviruses. Infected HeLa cell monolayers were incubated for 3 days at 37°C and stained with crystal violet.

4028T.V mutants were examined in one-step growth experiments (Fig. 2). As in the wild-type infection, virus progeny was initially detected at approximately 3 h p.i. within mutant-infected cells and reached maximum levels between 5 and 6 h p.i. However, consistent with the small-plaque phenotype, the yield of infectious virus per cell was reduced approximately 5- and 10-fold on infection with the 4028T.S and 4028T.V mutants, respectively. Overall levels of mutant viral RNA, protein synthesis, and myristoylation were comparable to those after infection with the wild-type virus (data not shown).

We examined the profiles of synthesized proteins in lysates from mutant- and wild-type-infected cells that were metabolically labeled with [^{35}S]methionine (Fig. 3, lanes 1 to 3). All prominent viral proteins, except for capsid protein VP2, were observed with normal stoichiometries. Thus, shutdown of host protein synthesis and overall viral protein synthesis appeared unaffected in these mutants. Concentrations of VP2 were reduced relative to those of other viral capsid proteins within the mutant lysates. In addition, in 4028T.V-infected cell lysates, a slight increase in P1 and 1ABC bands was also reproducibly detected. VP2 and 1ABC proteins are generated by proteolytic cleavage of P1 during poliovirus capsid assembly. These results indicated that substitutions at the 4028T residue affect capsid assembly and consequently limit the final yield of mature virus. Poliovirus assembly intermediates contain identical protein subunits (VP0-VP3-VP1). Thus it is impossible to determine the

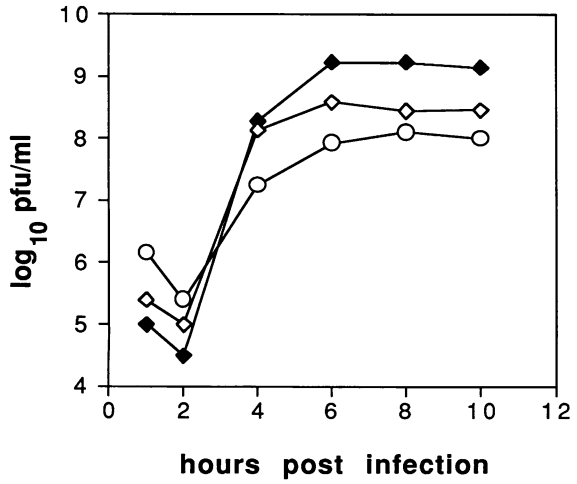

FIG. 2. Single-step growth curves of wild-type (◆), 4028T.S (◇), and 4028T.V (○) viruses. Infected HeLa cells (MOI, 10) were grown in suspension at 37°C. Aliquots were removed at various times, and titers were determined by plaque assays.

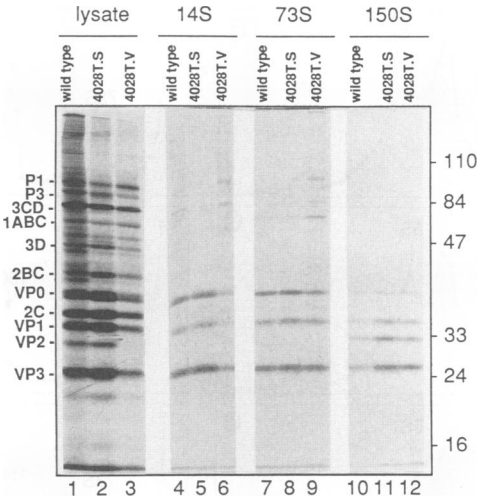

FIG. 3. Electrophoretic analysis of [^{35}S]methionine-labeled wild-type, 4028T.S, and 4028T.V viral proteins. Cells were infected with wild-type (lanes 1, 4, 7, and 10), 4028T.S (lanes 2, 5, 8, and 11) or 4028T.V (lanes 3, 6, 9, and 12) viruses. Infected-cell lysates (lanes 1 to 3) were fractionated on sucrose gradients, and the 14S pentamer (lanes 4 to 6), 73S empty capsid (lanes 7 to 9), and 150S mature virus (lanes 10 to 12) fractions were separated on SDS–10% polyacrylamide gels. Viral proteins are identified on the left. The migration of prestained markers (Bio-Rad) is indicated on the right.

nature of the capsid assembly defect by examining the protein profiles present in unfractionated 4028T.S- or 4028T.V-infected cell lysates. Separation of the assembly intermediates on sucrose gradients revealed substantial differences in the assembly of 4028T.S and 4028T.V.

The assembly intermediates present in 4028T.S- and 4028T.V-infected cell extracts were compared with those observed in wild-type-infected cells. Lysates, continuously labeled with [^{35}S]methionine, were loaded onto 6 to 25% sucrose gradients to separate the monomer (5S) and pentamer (14S) intermediates and onto 15 to 30% sucrose gradients to separate empty capsids (73S) and mature virions (150S) (Fig. 4). As expected for wild-type-infected cells, most of the label was found in the 5S monomer and mature 150S virion fractions. However, pentamer, and empty capsid assembly intermediates were clearly evident in wild-type-infected cell lysates. Labeled nonstructural proteins sediment within the 2S to 4S region of the gradients. Consistent with its small-plaque phenotype, the number of mature virus particles observed in 4028T.S-infected cell lysates was severely reduced. Concomitant with the reduction of mature virus was an apparent increase in the steady-state levels of pentamer intermediates in 4028T.S mutant-infected cells. Although not depicted in this particular set of gradients, increased levels of empty capsid were also occasionally observed. Examination of 4028T.S mutant 14S pentamer and 73S empty capsid fractions revealed that P1, VP0, VP3, and VP1 proteins of the correct molecular weights and stoichiometries were observed in each assembly intermediate fraction (Fig. 3, lanes 5 and 8). Thus the observed accumulation of pentamers in 4028T.S-infected cell lysates was not due to incorrect processing of the P1 precursor by the 3CD protease, leading to defects in capsid assembly. Similarly, analysis of assembly intermediates present in 4028T.V-infected cell extracts revealed the presence of monomer, pentamer, and empty capsid intermediates (Fig. 4e and f). However, an

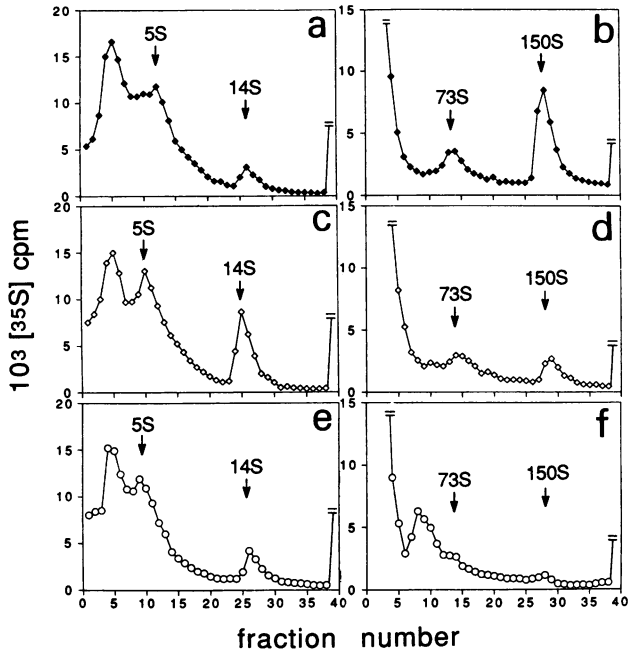

FIG. 4. Sucrose density gradient analyses of assembly intermediates from wild-type- (a and b), 4028T.S- (c and d), or 4028T.V (e and f)-infected HeLa cells. Viral proteins were metabolically labeled continuously with [^{35}S]methionine between 3.5 and 5.5 h p.i. Equal volumes of extracts were loaded on 6 to 25% (panels a, c, and e) or 15 to 30% (panels b, d, and f) linear sucrose gradients. The sedimentation direction is from left to right. The positions and the sedimentation values of the intermediates are indicated.

additional species accumulated in mutant-infected cells, and this species sedimented between the mutant pentamer and empty capsid intermediates (with an estimated value between 50S and 60S). Sodium dodecyl sulfate-polyacrylamide gel electrophoresis (SDS-PAGE) analysis of this complex showed that VP0, VP3, and VP1 were present in normal proportions, indicating that this 50S to 60S species was an assembly product. Thus, both serine and valine mutants display defects in the capsid assembly pathway, but the defects appear to be distinctly different.

The conformational stability of 4028T.S intermediates is altered. Increased concentrations of mutant assembly intermediates could reflect a more rapid formation or a slower exit of the capsid proteins from these assembly compartments. Thus, the kinetics of virus assembly in 4028T.S mutant- and wild-type-infected cells were analyzed by labeling with [^{35}S]methionine for 1 h and subsequently chasing with excess cold methionine (Fig. 5). Although the mature virion and the 5S monomers were the major species present at the end of the labeling period, as expected, all assembly intermediate forms were present within wild-type-infected cells. Over the chase period, the label moved from the 5S monomer compartment into the obligate 14S pentamer compartment and subsequently into the 73S empty capsid and 150S mature virion compartments. In contrast, within 4028T.S mutant-infected cells at the end of the labeling period, the monomer and pentamer intermediates were the major labeled species (Fig. 5B). Over the chase period, label moved out of the 5S monomer compartment with the same kinetics as that observed in wild-type-infected cells. Thus, the kinetics of pentamer formation from the 4028T.S monomers appeared similar to those observed with wild-type 5S monomers. However, label moved out of the mutant pentamer compartment with substantially slower kinetics than for the wild type. This suggested that the formation of empty capsids and mature virions from pentamer intermediates was inhibited in mutant-infected cells. The transient increase in mutant pentamers observed after a 1-h chase period was consistent with formation of pentamer intermediates at normal kinetics and with inhibition of the formation of higher-order intermediates from pentamers.

The noncompetence of mutant pentamers to assemble further into empty capsids was also observed in an in vitro assembly assay at 37°C to form empty capsids (80S) (17). Wild-type and mutant pentamers (14S fractions) were isolated at 4°C and incubated at 37°C for 1 h. The resultant empty capsids were separated from the parental pentamers on sucrose gradients (Fig. 6). Approximately 85% of the wild-type pentamers assembled into empty capsids with expected sedimentation value of 80S. In contrast, less than 20% of the sucrose-purified 4028T.S mutant pentamers assembled into structures that sediment at 80S; heterogeneous aggregates of unknown pentamer stoichiometries appear to be formed (Fig. 6B). Thus two populations of pentamers appear to be present within mutant-infected cells—an assem-

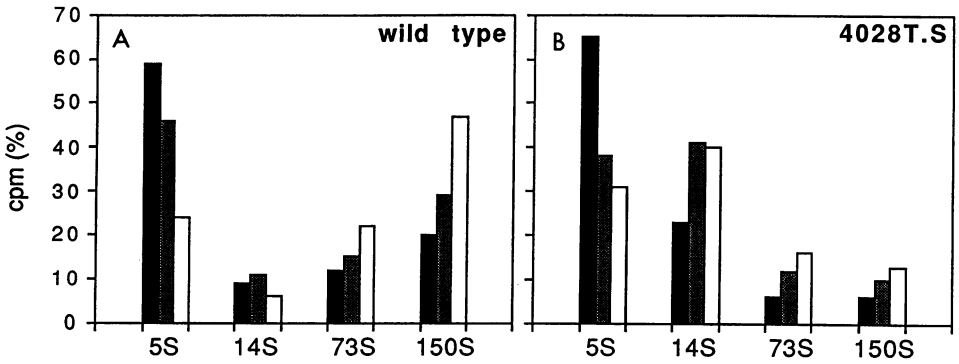

FIG. 5. Kinetics of wild-type (A) and 2048T.S (B) virion assembly. Viral proteins were pulse-labeled with [^{35}S]methionine (40 μCi/ml) from 3 to 4 h p.i., and subsequently a large excess of cold methionine was added to the media. Aliquots were removed after the pulse period at 4 h p.i. (■), 5 h p.i. (▩), and 6 h p.i. (□). Infected cells were lysed, and the assembly intermediates were separated on sucrose gradients. The amount of label (cpm) present in each assembly compartment was determined and is expressed as a percentage of total capsid proteins.

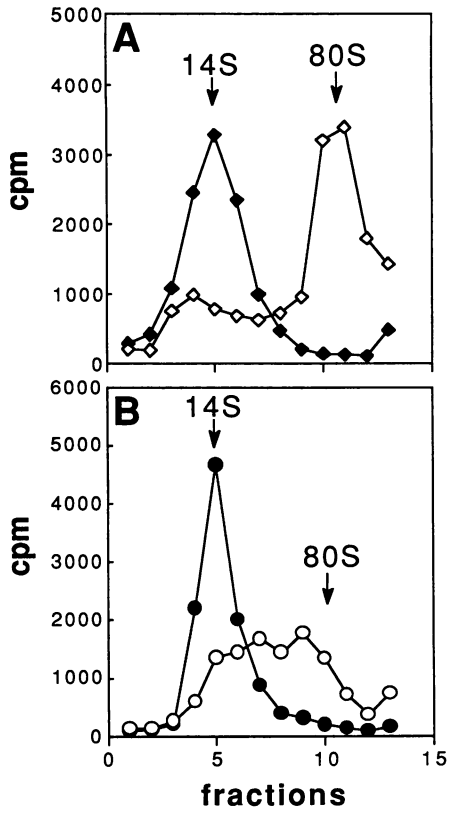

FIG. 6. In vitro assembly of purified pentamers. Sucrose-purified pentamers (14S) from wild type- (◆, ◇) or 4028T.S (●, ○)-infected cells in TNM buffer were incubated at either 4°C (solid symbols) or 37°C (open symbols) for 1 h. Samples were analyzed subsequently on 10 to 30% sucrose gradients. The sedimentation direction is from left to right.

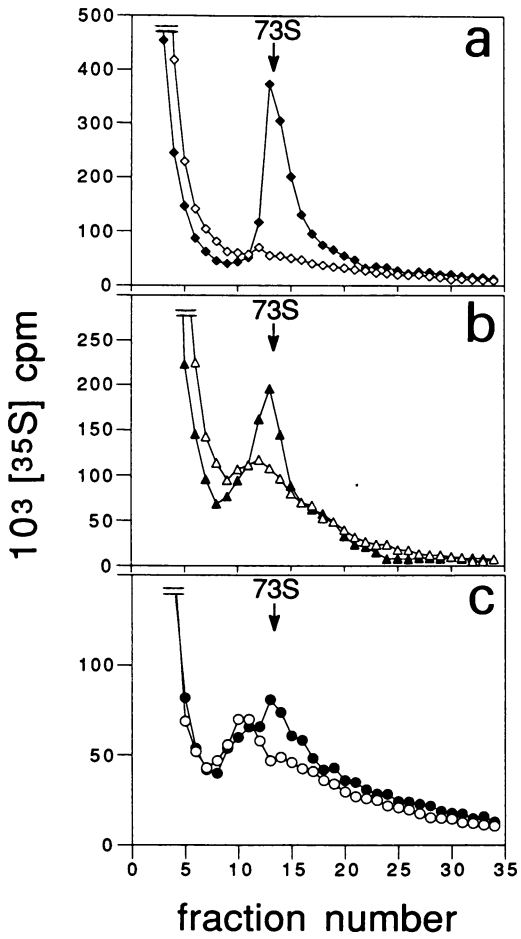

FIG. 7. pH-induced dissociation of empty capsids. HeLa cells were infected with wild-type (◆, ◇), 4028T.S (▲, △) or 4028T.V (●, ○) virus and incubated at 37°C. Cells were lysed at either pH 7.5 (solid symbols) or pH 8.3 (open symbols) and analyzed on 15 to 30% sucrose gradients.

bly-inactive complex and an assembly-active structure that could proceed to form empty and mature virions.

Previous studies have identified two species of empty capsids differing in antigenic properties and their dissociability at pH 8.3 (13, 16). Antigenically native empty capsids can dissociate to pentamers at pH 8.3, and the resultant dissociated pentamers can be reassembled into empty capsids upon acidification. Nonnative antigenic empty capsids are not dissociable and appear to be analogous antigenically to the heat-inactivated virus particle. In vivo, wild-type assembly-competent empty capsid intermediates will reversibly disassemble into pentamers, and this dissociability can be discerned in vitro by raising the pH of the cell lysate from 7.3–7.5 to 8.3–8.5 (13, 16). Thus, the assembly competence of the empty capsid structures formed within 4028T.S mutant-infected cells could be estimated in vitro by their dissociability at pH 8.3. Infected cells were lysed at either pH 7.5 or 8.3, and the assembly intermediates were analyzed on sucrose gradients (Fig. 7). As expected, wild-type empty particles were totally dissociated at the higher pH. In contrast, approximately 25% of the empty capsid population present in 4028T.S-infected cells was not dissociable (Fig. 7b). These results showed that the empty capsids generated in vivo from the assembly-active 4028T.S pentamer subpopulation also existed as two biochemically distinguishable populations—a fraction which is pH stable and therefore not assembly active, and one which is pH dissociable and assembly active (like the wild type) and which presumably proceeds to yield mature virions. Thus the in vivo and in vitro data both indicate that at each postpromoter assembly stage, assembly-inactive and assembly-active 4028T.S intermediates are present and that they presumably differ in their structural conformations. This suggests that the 4028T.S mutant assembly intermediates are conformationally more unstable and that the biochemical phenotypes observed result from the inability to maintain an assembly-competent conformation required for empty-capsid and mature-virion formation.

4028T.V 50S to 60S postpentamer complexes appear assembly inactive. A 50S to 60S species is observed in 4028T.V mutant-infected cells but not in wild-type-infected cells. Accumulation of this 50S to 60S species could result from an increase in the half-life of a highly transient intermediate that normally occurs during assembly of the wild-type virion particle. Alternatively, defective assembly of mutant pentamers could generate 60S "dead-end" products that are no longer assembly competent. Therefore, infected cells were pulse-labeled with [^{35}S]methionine and subsequently chased with cold methionine, and the fate of the labeled 60S species was monitored over the chase period (Fig. 8). Although some movement of label from the 60S peak and eventually

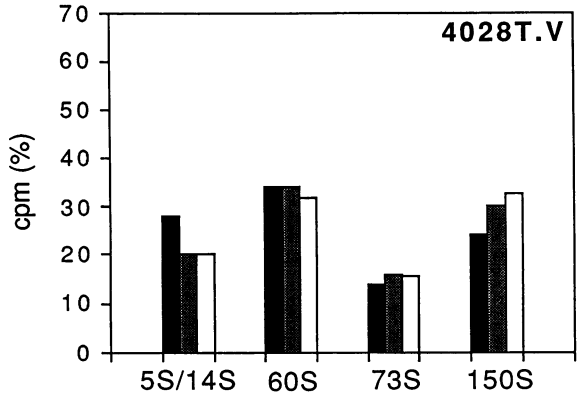

FIG. 8. Fate of the 4028T.V 60S assembly complex. Viral proteins were labeled at 3 h p.i. with [^{35}S]methionine, and cold methionine was added to the infection at 4 h p.i. Aliquots of infected cells were removed at 4.5 h p.i. (■), 5.25 h p.i. (▩), and 6 h p.i. (□). Cells were lysed, and the lysates were analyzed on sucrose gradients. The radioactivity (cpm) in each assembly compartment (identified by their sedimentation values) is expressed as a percentage of the total label associated with the capsid proteins.

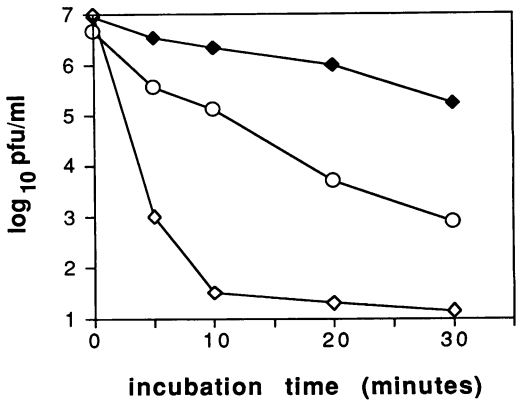

FIG. 9. Temperature-induced inactivation of purified wild-type (◆), 4028T.S (◇), and 4028T.V (○) viruses. Virus (10^7 PFU/ml of PBS) was incubated at 45°C, and aliquots were removed at various times. The titer of infectious virus remaining in each aliquot was determined.

into the 150S virion peak was observed, most of the label remained in the 60S compartment over the 2-h chase period. Although it cannot be excluded that the 60S species may be a population of assembly-active intermediates whose normally transient half-life has been increased by the valine substitution, the small amount of label that left the 60S compartment suggested that only a small fraction of the 60S species was assembly active. In addition, approximately 20% of the empty capsids (73S) were not dissociable at pH 8.3 (Fig. 7c), indicating that again a fraction of the empty capsids assembled in 4028T.V-infected cells were not assembly active. Thus the overall reduction of 4028T.V mature virus yield appeared to be due to accumulation of a 60S assembly intermediate and, to a lesser extent, to accumulation of non-assembly-competent empty capsids.

Characterization of assembled mutant serine and valine particles. Replacement of threonine 28 with either serine or valine affects specific steps of virus assembly and results in a significant reduction of mature virus yield (5- to 10-fold). However, a significant fraction of the synthesized capsid proteins are assembled into mature virus particles and lead to the generation of viable viral mutants. The structures of the assembled particles were probed to determine whether these substitutions also caused changes in the virion or had additional consequences on virus viability. Like the wild-type particle, 4028T.S and 4028T.V mutant particles were stable to detergent and high-ionic-strength environments. In addition, the labeled proteins within mutant virions were not found to be more sensitive than the wild type to either trypsin or V8 protease. Finally, MAbs to each of the major neutralizing antigenic sites on the surface of serotype 1 strains (sites 2, 3A, and 3B) will bind mutant virions (data not shown). These data indicate that the external physical structure of the mutant virions (and presumably the overall organization and folding of the capsid proteins within the particle) is not significantly altered by the substitutions at threonine 28, a residue that is located within the particle interior, near the inner surface of the virion shell.

Mutant infectivity is more sensitive to agents inducing conformational transitions. By several criteria, the overall physical structure of the assembled mutant virions appeared to be biochemically identical to that of wild-type virion. However, slight differences in viral infectivity were consistently observed. Although values for the particle/PFU ratios varied for different preparations, within any given preparation the particle/PFU ratio of the serine mutant was always higher than that of the valine mutant and both ratios were always higher than that of the wild-type virus. Thus the relative infectivity of these viral strains can be represented in the order 4028T > 4028T.V > 4028T.S, with the serine and valine mutants being approximately 2- to 3-fold and 1.5- to 2-fold, respectively, less infectious than wild-type virus (data not shown).

Simple inefficiency in assembly is insufficient to account for the observed increase in particle/PFU ratios. An alternative mechanism which would be consistent with this observed increase would be a decrease in the stability of the assembled products. Viral infectivity is lost on incubation at 45°C. Further studies have demonstrated that this loss of infectivity is due to conformational alterations within the wild-type virion particle (6). Thus, the thermal sensitivities of 4028T.S and 4028T.V viruses were compared with that of the wild-type virus (Fig. 9). Mutant viral infectivity was much more sensitive to thermal inactivation than was the infectivity observed with wild-type virus. Dramatically, 4028T.S infectivity decreased 7 $\log_{10}$ units within 10 min and 4028T.V lost 4 $\log_{10}$ units of infectivity within 30 min. In contrast, the wild type lost only 1 to 2 $\log_{10}$ units of infectivity over 30 min. Consistently, the 4028T.S mutant was substantially more sensitive than 4028T.V mutant to thermal inactivation. These results suggested that threonine 28 participated in interactions that contribute to the structural integrity of the infectious virion; modification of these interactions (by substitution of different amino acid residues) led to greater loss of viral infectivity on incubation at 45°C.

The apparent structural lability of the mutant virions is also reflected by their sensitivity to antibody neutralization. Serial dilutions of MAbs for the antigenic sites 3A (MAbs 1 and 12), 3B (MAbs 10 and 13) and 2 (MAbs 4 and 8) (15) were used in microneutralization assays, and the effective titers necessary to neutralize 5×10^4 PFU was determined (Table 1). Although all antibodies recognized the mutant and wild-type viruses, lower dilutions of virtually all MAbs were required to neutralize equivalent PFU of wild-type virus

TABLE 1. Neutralization of 4028T.S and 4028T.V poliovirus mutants by MAbs[a]

Virus[b]	Neutralizing titer[c] with MAb:					
	1	12	10	13	4	8
Wild type	1:2,000	1:50	1:200	1:100	1:500	1:20
4028T.S	1:8,000	1:100	1:3,200	1:1,200	1:32,000	1:320
4028T.V	1:4,000	1:50	1:1,600	1:600	1:8,000	1:160

[a] The MAbs recognize the three major neutralizing sites for serotype 1 poliovirus. MAbs 1 and 12 recognize antigenic site 3A; MAbs 10 and 13 recognize antigenic site 3B; and MAbs 4 and 8 recognize antigenic site 2 (15).
[b] Viruses were purified on CsCl density gradients.
[c] Neutralizing titers were determined by microneutralization assay. The values represent the highest dilution of the MAb still able to protect HeLa cells from the viral infection.

than of either mutant; the effective neutralizing titers were reproducibly and consistently higher when measured with the mutant than with the wild-type viruses. Thus the number of neutralization antibodies per infectious particle is smaller for both mutants than for the wild-type parent. Moreover, given that the particle/PFU ratio is increased in these mutants, the ratio of antibodies to viral particles is even lower for each mutant than for the wild type. It is thought that MAbs neutralize viral infectivity either by preventing the conformational transitions necessary to initiate successful infection or by actively inducing structural changes that result in virus inactivation. Although the mechanisms by which these antibodies neutralize viral infectivity are unknown, the increased titers, together with the decreased particle stability at high temperature, suggest that the assembled mutant particle is functionally more unstable than the wild type.

DISCUSSION

Viable poliovirus mutants are obtained on replacement of threonine 28 with either one of the two amino acids, serine or valine, whose side chains have functional groups in common with the parental threonine residue. These mutants, when compared with the wild-type virus, show qualitatively similar phenotypes—accumulation of assembly-inefficient or incompetent postmonomer assembly intermediates and decreased infectivity and stability of the assembled mutant virus particles. Thus, threonine 28 of capsid protein VP4 participates in chemical interactions that appear relevant at several stages in the life cycle of the viral capsid, stabilizing both the assembly-competent conformations of postmonomer capsid intermediates and the infection-competent structure of the assembled particles.

Despite the general similarities observed, each mutant displays distinguishing phenotypes; i.e., assembly of the serine and valine mutants is apparently affected at different stages, and the assembled serine particles are quantitatively more sensitive than the valine mutant to conformational perturbations. These distinctive phenotypes coupled with the different chemical properties of the serine and valine side chain suggest that the hydroxyl and methyl groups of threonine 28 provide specific but different interactions which are relevant for the efficient assembly and overall stability of the poliovirus capsid. The viability of both serine and valine mutants suggests that assembly, conformational stability, and proper biological function of the capsid are not dependent on the presence of both the hydroxyl- and methyl-mediated interactions of threonine 28. However, the lethality of the glycine substitution indicates that the presence of either set of interactions is required.

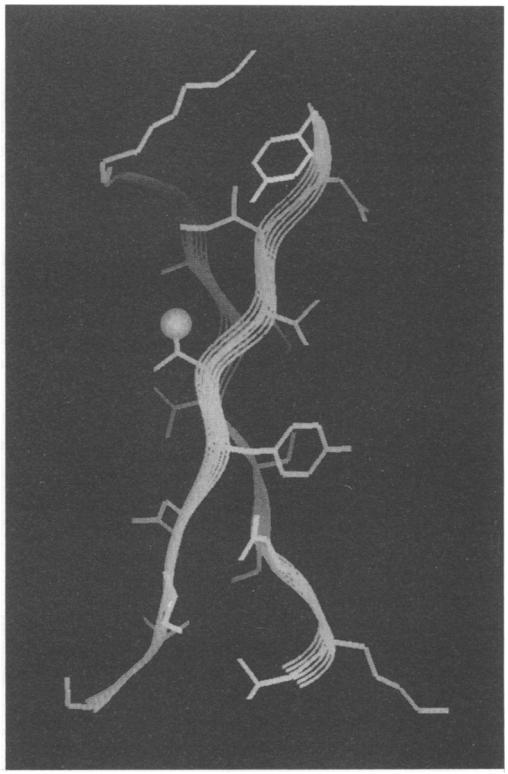

FIG. 10. Structural environment of Thr-28. The two-stranded antiparallel β-sheet structure in VP4 of one capsid protomer (VP4 residues 2 to 10 and 23 to 32) is displayed. Portions of the structure that are closer to the viewpoint are lighter than portions which are further away. The topologies of the alpha carbon backbone in the two strands are depicted as ribbons, with the positions of individual side chains projecting from the ribbon. Myristate modification of Gly-2 is located on the back strand of the β-sheet at the upper left corner. Cpk volumes for the methyl moiety of Thr-28 were calculated from the atomic model, and the surface of this volume (scaled to 0.3 of actual) is displayed.

Threonine 28 is important for the structure of the fully assembled virus. At fivefold axes within the virus particle, the threonine hydroxyl group is hydrogen bonded to the carbonyl oxygen of the myristoyl moiety from an adjacent symmetry-related VP4. In addition, detailed examination of the surrounding environment reveals that this threonine 28 also is part of a two-stranded anti-parallel β-sheet structure (4, 5). The methyl group of the threonine is surrounded by a completely hydrophobic environment (Fig. 10). It appears to be in Van der Waals contact with the side chains of other β-sheet related residues (4003A, 4005V, and 4030I) from the same subunit and with the myristoyl hydrocarbon of the neighboring subunit. Thus, both the hydroxyl and methyl substituents of threonine 28 appear to provide interactions that stabilize the particle structure.

The general phenotypes observed for the 4028T.S and 4028T.V viruses indicate that these stabilizing interactions, observed in the static view provided by the virus structure, are functionally important. Both mutant viruses are significantly less infective than the wild-type virus and are substantially more sensitive to thermal inactivation or antibody neutralization. These phenotypes may result from perturbations of the threonine 28-mediated interactions found in the

structure. Although the methyl group would be available to participate in the β-sheet interactions, replacement of the hydroxyl group with a methyl group (as occurs in the valine mutant) would destroy the intersubunit threonine-myristate hydrogen bond. Moreover, this additional methyl group is too close to the myristoyl carbonyl oxygen for the preferred rotomer configurations and is sterically strained. Thus, rearrangements during virion assembly and within the assembled particle must occur to compensate for the presence of the additional methyl group and to maintain viral viability. The presence of these structural compensations is also suggested by small but detectable increase in the concentrations of P1 (the capsid precursor) and 1ABC (a cleavage intermediate of P1) found in 4028T.V but not 4028T.S mutant-infected cells. These are most evident as increases in the amount of higher-molecular-weight material present in the 14S and 73S peaks (Fig. 1). Although the absolute amounts of the processing intermediates vary between infections, these increases indicate that proteolytic processing of 4028T.V P1 protein may be slightly slower or less efficient and may result from slight differences (induced by the valine substitution) in the mutant P1 structure. Removal of the methyl group (as occurs with the serine mutant) would result in the loss of potentially stabilizing methyl β-sheet interactions and would create a "hole" within the center of this neighboring hydrophobic cluster. This void would presumably be filled by structural compensations within the virus. Because structural changes on the external surfaces of the mutant viruses were not detected by several different biochemical probes, these rearrangements for both serine and valine mutants are likely to be localized within the capsid interior near the fivefold axes. Further structural studies of these mutants are required to define these local rearrangements and to relate these predicted structural changes to the phenotypes of the assembled mutant particles.

Within the virion, threonine 28 forms intersubunit interactions with residues from other fivefold-symmetry-related VP4 proteins. Thus these intersubunit interactions cannot exist until monomer subunits are assembled into pentamers. The general observation that the assembly defective phenotypes of both mutants appear to affect postmonomer assembly stages is consistent with these structural observations.

Substitution of serine for threonine results in accumulation of pentamers. Although some of the 4028T.S pentamers will proceed and assemble into mature virus, most of them appear unable to do so. This suggests that most pentamers are assembly inactive and lack the proper conformation necessary for efficient progression to the next stage of the assembly process. Thus, interactions involving the methyl group of threonine 28 directly or indirectly maintain the pentamers in a conformation which is required for assembly into postpentamer structures (empty capsid and mature virion).

Accumulation of a highly long-lived 50S to 60S assembly product is observed on replacement of threonine 28 with a valine residue. A capsid intermediate with a sedimentation value of 55S has been identified previously as a short-lived assembly product of 14S subunits (3). This 55S intermediate appears to be the precursor of the empty capsid (73S) and virion and is hypothesized to be a hemicapsid structure. It is possible that the 50S to 60S intermediate found in 4028T.V mutant-infected cell extracts is a similar assembly complex, whose structure, on replacement of the threonine with valine, is highly stable and is retained in the 55S compartment. Alternatively the observed 50S to 60S material may be formed by mutant pentamer complexes with an abortive organization which is totally different from the hemicapsid structure suggested for the 55S species. Further characterization of both wild-type 55S and mutant 50S to 60S species is necessary to resolve the position and relevance of these complexes within the assembly pathway.

ACKNOWLEDGMENTS

We thank D. J. Filman for assistance in the structural analysis and R. Grant and J. Hogle for critical discussions and assistance with Fig. 10.

This work was supported by Public Health Service grant AI122627 from NIH and by research grant MV-466 from the American Cancer Society.

REFERENCES

1. **Chow, M., and D. Baltimore.** 1982. Isolated poliovirus capsid protein VP1 induces a neutralizing response in rats. Proc. Natl. Acad. Sci. USA **79**:7518–7521.
2. **Chow, M., J. F. E. Newman, D. Filman, D. M. Hogle, D. J. Rowlands, and F. Brown.** 1987. Myristylation of picornavirus capsid protein VP4 and its structural significance. Nature (London) **327**:482–486.
3. **Corrias, M. V., O. Flore, E. Broi, M. E. Marongiu, A. Pani, S. Torelli, and P. La Colla.** 1987. Characterization and role in morphogenesis of a new subviral particle (55 S) isolated from poliovirus-infected cells. J. Virol. **61**:561–569.
4. **Filman, D. J., R. Syed, M. Chow, A. J. Macadam, P. D. Minor, and J. M. Hogle.** 1989. Structural factors that control conformational transitions and serotype specificity in type 3 poliovirus. EMBO J. **8**:1567–1579.
5. **Flore, O., C. E. Fricks, D. J. Filman, and J. M. Hogle.** 1990. Conformational changes in poliovirus assembly and cell entry, p. 429–438. *In* J. M. Hogle (ed.), Seminars in virology, vol. 1. The W. B. Saunders Co., Philadelphia.
6. **Fricks, C. E., and J. M. Hogle.** 1990. Cell-induced conformational change in poliovirus: externalization of the amino terminus of VP1 is responsible for liposome binding. J. Virol. **64**:1934–1945.
7. **Hogle, J. M., M. Chow, and D. J. Filman.** 1985. Three-dimensional structure of poliovirus at 2.9 Å resolution. Science **229**:1358–1365.
8. **Jacobson, M. F., and D. Baltimore.** 1968. Morphogenesis of poliovirus. I. Association of the viral RNA with coat proteins. J. Mol. Biol. **33**:369–378.
9. **Laemmli, U. K.** 1970. Cleavage of structural proteins during the assembly of the head of bacteriophage T4. Nature (London) **227**:680–685.
10. **Lee, Y. M., and M. Chow.** 1992. Myristate does not function as a membrane association signal during poliovirus capsid assembly. Virology **187**:814–820.
11. **Marc, D., G. Drugeon, A. Haenni, M. Girard, and S. van der Werf.** 1989. Role of myristoylation of poliovirus capsid protein VP4 as determined by site-directed mutagenesis of its N-terminal sequence. EMBO J. **8**:2661–2668.
12. **Marc, D., G. Masson, M. Girard, and S. van der Werf.** 1990. Lack of myristoylation of poliovirus capsid polypeptide VP0 prevents the formation of virions or results in the assembly of noninfectious virus particles. J. Virol. **64**:4099–4107.
13. **Marongiu, M. E., A. Pani, M. V. Corrias, M. Sau, and P. L. Colla.** 1981. Poliovirus morphogenesis. I. Identification of 80S dissociable particles and evidence for the artifactual production of procapsids. J. Virol. **39**:341–347.
14. **Moscufo, N., J. Simons, and M. Chow.** 1991. Myristoylation is important at multiple stages in poliovirus assembly. J. Virol. **65**:2372–2380.
15. **Page, G. S., A. G. Mosser, J. M. Hogle, D. J. Filman, R. R. Rueckert, and M. Chow.** 1988. Three-dimensional structure of poliovirus serotype 1 neutralizing determinants. J. Virol. **62**: 1781–1794.
16. **Putnak, J. R., and P. A. Phillips.** 1982. Poliovirus empty capsid

morphogenesis: evidence for conformational differences between self- and extract-assembled empty capsids. J. Virol. **41:**792–800.

17. **Rombaut, B., A. Foriers, and A. Boeye.** 1991. In vitro assembly of poliovirus 14 S subunits: identification of the assembly promoting activity of infected cell extracts. Virology **180:**781–787.
18. **Rueckert, R. R.** 1990. Picornaviridae and their replication, p. 507–548. *In* B. N. Fields, D. M. Knipe, R. M. Chanock, M. S. Hirsch, J. L. Melnick, T. P. Monath, and B. Roizman (ed.), Virology, 2nd ed. Raven Press, New York.
19. **Sanger, F., S. Nicklen, and A. R. Coulson.** 1977. DNA sequencing with chain-terminating inhibitors. Proc. Natl. Acad. Sci. USA **74:**5463–5467.
20. **Sayers, J. R., W. Schmidt, and F. Eckstein.** 1988. 5′-3′ exonucleases in phosphorothioate-based oligonucleotide-directed mutagenesis. Nucleic Acids Res. **16:**791–802.
21. **Simons, J., C. Reynolds, N. Moscufo, L. Curry, and M. Chow.** 1990. Myristylation of poliovirus VP4 capsid proteins, p. 158–165. *In* M. A. Brinton and F. X. Heinz (ed.), New aspects of positive-strand RNA viruses. American Society for Microbiology, Washington, D.C.